



Research article

Energy-to-peak control for switched systems with PDT switching

Jingjing Dong¹, Xiaofeng Ma¹, Lanlan He¹, Xin Huang^{2,*} and Jianping Zhou¹

¹ School of Computer Science and Technology, Anhui University of Technology, Ma'anshan 243032, China

² Institute of Automation, Jiangnan University, Wuxi 214122, China

* **Correspondence:** Email: xhuang.js@gmail.com.

Abstract: This paper investigates the issue of energy-to-peak control for continuous-time switched systems. A generalized switching signal, known as persistent dwell-time switching, is considered. Two different strategies for state-feedback controller design are proposed, using distinct Lyapunov functions and a few decoupling techniques. The critical distinction between these two strategies lies in their temporal characteristics: one is time-independent, while the other is quasi-time-dependent. Compared to the former, the latter has the potential to be less conservative. The validity of the proposed design strategies is demonstrated through an example.

Keywords: switched systems; persistent dwell time; energy-to-peak control

1. Introduction

Switched systems (SSs) are a significant subclass of hybrid systems consisting of a series of subsystems and a signal for controlling the switch among them [1]. Over the last few decades, SSs have been applied in various domains, such as DC-DC power converters [2], inverter circuits [3], unmanned vehicles [4], secure communication [5], fault estimation [6] and image encryption [7]. At the same time, stability analysis and controller design for SSs, as fundamental issues in the control area, have been intensively studied and a significant amount of results have been proposed in the international literature; see, e.g., [8–16].

The stability of an SS is dependent on each subsystem and highly affected by the switching frequency. Although all subsystems are asymptotically stable (AS), the entire SS may have a non-convergent solution trajectory caused by fast switching [17]. However, the stability can be maintained when the switching is sufficiently slow in the sense that the running time of each active subsystem is not less than a specified threshold called the dwell time (DT) [18]. Actually, this is also true even when fast switching occurs occasionally, as long as the average dwell time (ADT) is long enough [19].

In 2004, a type of switching signal, called the persistent DT (PDT) switching signal, was introduced in [20] to represent the switching signal that has infinitely many intervals of length no less than a given positive constant ε (i.e., the PDT) during which no switch occurs, and distance between two consecutive intervals with this property does not surpass a period of persistence δ . As explained in [20], the PDT switching is more common and suitable than DT and ADT switching for describing switching phenomena associated with hybrid systems.

There have been various control strategies, including uniform tube-based control [21], fault-tolerant control [22], quasi-synchronization control [23], quantized fuzzy control [24], \mathcal{L}_1 finite-time control [25], dynamic output-feedback control [26], sliding mode control [27] and model predictive control [28], that have been introduced for discrete-time SSs with PDT switching over the past few years. To the best of our knowledge, however, there are no available reports on the energy-to-peak control of continuous-time SSs (CTSSs) with PDT switching. Energy-to-peak control can guarantee that the infinity norm of the controlled output is less than a certain disturbance attenuation level [29]. In many practical situations, such a control approach serves as an appropriate selection for system design because it is insensitive to specific statistical characteristics of the noise signals and exhibits good robustness [30].

In this paper, we are interested in the energy-to-peak control for CTSSs with PDT switching. Our objective is to ensure that the CTSS is AS with a certain energy-to-peak disturbance-attenuation performance (EPDAP) level [31]. We first introduce a lemma regarding the asymptotic stability and EPDAP analysis of the PDT-based CTSS. Then, we propose a time-independent state-feedback controller design approach using a Lyapunov function (LF) and decoupling techniques. To reduce conservatism, we further present a quasi-time-dependent (QTD) controller design method. The required gains of these two types of controllers can be obtained by means of feasible solutions of linear matrix inequalities (LMIs), which are known to be easily solved with available tools in MATLAB [32]. Finally, we give an example to illustrate the effectiveness of our controller design strategies.

Notation: We denote by \mathbb{R}^n the n -dimensional Euclidean space, by \mathbb{Z}_+ the set of non-negative integers, by \mathbb{R} the set of real numbers, by $\|\cdot\|$ the 2-norm, and by $\lfloor \cdot \rfloor$ the round-down operator. We apply an asterisk “*” to represent a symmetric term in a matrix and the superscript “ T ” to stand for the transpose operator. For any square matrix X , we utilize $X > 0$ (< 0) to imply that the matrix is symmetric positive-definite (negative-definite) and define $\mathcal{S}(X)$ as $X + X^T$. Moreover, we let \mathcal{K}_∞ be a class of continuous and strictly increasing functions $\beta(\cdot)$ that satisfy $\beta(0) = 0$.

2. Preliminaries

In the field of control for SSs with PDT switching, the majority of published work primarily focuses on the discrete-time setting; see, e.g., [21–28]. In this paper, we will consider CTSSs with PDT switching as in [33, 34]. The system model is described by

$$\dot{\psi}(t) = A_{\zeta(t)}\psi(t) + B_{\zeta(t)}u(t) + E_{\zeta(t)}\varpi(t), \quad (2.1a)$$

$$\phi(t) = G_{\zeta(t)}\psi(t), \quad (2.1b)$$

within which $\psi(t) \in \mathbb{R}^n$, $\phi(t) \in \mathbb{R}^p$ and $u(t) \in \mathbb{R}^q$ stand for the state, controlled output and control input, respectively; $\varpi(t) \in \mathbb{R}^r$ denotes the exterior disturbance that belongs to $\mathcal{L}_2[0, \infty]$ [35]; $A_{\zeta(t)}$, $B_{\zeta(t)}$, $E_{\zeta(t)}$ and $G_{\zeta(t)}$ are the given system matrices; $\zeta(t)$ denotes the switching rule, which is a right-continuous

holds under $\psi(0) = 0$, where $\|\phi(t)\|_\infty = \sup_{t \geq 0} \|\phi(t)\|$.

Before ending the section, we state three preliminary propositions that we are going to use to prove our main results.

Proposition 1. [37] Given a scalar $\rho > 0$ and two locally integrable functions $\mathcal{V}(t)$ and $\Gamma(t)$ defined on $[0, \infty)$, if $\dot{\mathcal{V}}(t) \leq -\rho\mathcal{V}(t) + \Gamma(t)$ holds, then we obtain

$$\mathcal{V}(t) \leq e^{-\rho t} \mathcal{V}(0) + \int_0^t e^{-\rho(t-\sigma)} \Gamma(\sigma) d\sigma, \quad t \geq 0.$$

Proposition 2. [38] Given a real number η and real matrices \mathcal{X} , \mathcal{Y} , \mathcal{U} and \mathcal{W} ,

$$\begin{bmatrix} \mathcal{X} & * \\ \mathcal{U} - \eta\mathcal{W}\mathcal{Y} & \eta\mathcal{S}\{\mathcal{W}\} \end{bmatrix} < 0$$

holds if and only if both $\mathcal{X} < 0$ and $\mathcal{X} + \mathcal{S}\{\mathcal{Y}^T \mathcal{U}\} < 0$ hold true.

Proposition 3. [39] For any real matrices \mathcal{N}_1 , \mathcal{N}_2 and \mathcal{N}_3 ,

$$\begin{bmatrix} \mathcal{N}_1 & \mathcal{N}_2 \\ * & \mathcal{N}_3 \end{bmatrix} < 0$$

holds if and only if

$$\mathcal{N}_3 < 0 \text{ and } \mathcal{N}_1 - \mathcal{N}_2 \mathcal{N}_3^{-1} \mathcal{N}_2^T < 0.$$

3. Main results

We will give the following lemma, which provides a criterion for the analysis of the asymptotic stability and EPDAP.

Lemma 1. Given scalars $\delta \geq 0$, $\mu > 1$, $\rho > 0$, $\gamma > 0$ and $h_t > 0$, suppose that there is an LF $\mathcal{V}_{\mathcal{S}(t)}(\psi(t), t): (\mathbb{R}^n, \mathbb{Z}_+) \rightarrow \mathbb{R}$ and two classes of functions $\beta_1(\cdot)$, $\beta_2(\cdot) \in \mathcal{K}_\infty$ such that

$$\beta_1(\|\psi(t)\|) \leq \mathcal{V}_{\mathcal{S}(t)}(\psi(t), t) \leq \beta_2(\|\psi(t)\|), \quad (3.1)$$

$$\mathcal{V}_{\mathcal{S}(t)}(\psi(t), t) \leq \mu \mathcal{V}_{\mathcal{S}(t-r)}(\psi(t), t), \quad (3.2)$$

$$\dot{\mathcal{V}}_{\mathcal{S}(t)}(\psi(t), t) \leq -\rho \mathcal{V}_{\mathcal{S}(t)}(\psi(t), t) + \|\varpi(t)\|^2, \quad (3.3)$$

$$\|\phi(t)\|^2 \leq \gamma^2 \mathcal{V}_{\mathcal{S}(t)}(\psi(t), t) \quad (3.4)$$

hold. Then, for any PDT switching signal satisfying

$$\varepsilon \geq \frac{(\delta/h_t + 1) \ln \mu}{\rho} - \delta, \quad (3.5)$$

CTSS (2.1) is AS with the EPDAP level $\bar{\gamma} = \gamma \sqrt{\mu^{\delta/h_t + 1}}$.

Proof. Denote by $N(a, b)$ the count of switched times within any left-open time interval $(a, b]$. Then, for any $t \in [t_\kappa, t_{\kappa+1})$, $\kappa \in \mathbb{Z}_+$, one has

$$\mathcal{V}_{S(t)}(\psi(t), t) \leq \mu^{N(0,t)} e^{-\rho t} \mathcal{V}_{S(0)}(\psi(0), 0) + \int_0^t \mu^{N(\sigma,t)} e^{-\rho(t-\sigma)} \|\varpi(\sigma)\|^2 d\sigma. \quad (3.6)$$

Inequality (3.6) can be shown by mathematical induction. In fact, for $t \in (t_0, t_1)$ (i.e., $\kappa = 0$), using Proposition 1, one can get from (3.3) that

$$\begin{aligned} \mathcal{V}_{S(t)}(\psi(t), t) &= \mathcal{V}_{S(0)}(\psi(t), t) \\ &\leq e^{-\rho t} \mathcal{V}_{S(0)}(\psi(0), 0) + \int_0^t e^{-\rho(t-\sigma)} \|\varpi(\sigma)\|^2 d\sigma. \end{aligned}$$

Because of $N(\sigma, t) = 0$ for $\sigma \in [t_0, t)$, the inequality (3.6) obviously holds. For $t \in [t_1, t_2)$ (i.e., $\kappa = 1$), from (3.2) and (3.3), one can obtain

$$\begin{aligned} \mathcal{V}_{S(t)}(\psi(t), t) &= \mathcal{V}_{S(t_1)}(\psi(t), t) \\ &\leq e^{-\rho(t-t_1)} \mathcal{V}_{S(t_1)}(\psi(t_1), t_1) + \int_{t_1}^t e^{-\rho(t-\sigma)} \|\varpi(\sigma)\|^2 d\sigma \\ &\leq \mu e^{-\rho(t-t_1)} \mathcal{V}_{S(0)}(\psi(t_1), t_1) + \int_{t_1}^t e^{-\rho(t-\sigma)} \|\varpi(\sigma)\|^2 d\sigma \\ &= \mu e^{-\rho(t-t_1)} \{e^{-\rho(t_1-0)} \mathcal{V}_{S(0)}(\psi(0), 0) + \int_0^{t_1} e^{-\rho(t_1-\sigma)} \|\varpi(\sigma)\|^2 d\sigma\} + \int_{t_1}^t e^{-\rho(t-\sigma)} \|\varpi(\sigma)\|^2 d\sigma \\ &= \mu e^{-\rho t} \mathcal{V}_{S(0)}(\psi(0), 0) + \mu \int_0^{t_1} e^{-\rho(t-\sigma)} \|\varpi(\sigma)\|^2 d\sigma + \int_{t_1}^t e^{-\rho(t-\sigma)} \|\varpi(\sigma)\|^2 d\sigma \\ &= \mu^{N(0,t)} e^{-\rho t} \mathcal{V}_{S(0)}(\psi(0), 0) + \int_0^t \mu^{N(\sigma,t)} e^{-\rho(t-\sigma)} \|\varpi(\sigma)\|^2 d\sigma, \end{aligned}$$

which means that the inequality (3.6) is satisfied. Next, assume that (3.6) holds for $t \in [t_k, t_{k+1})$ ($k > 1, k \in \mathbb{Z}_+$). Then, one can write the following inequality:

$$\mathcal{V}_{S(t_k)}(\psi(t^*), t^*) \leq \mu^{N(0,t^*)} e^{-\rho(t^*-0)} \mathcal{V}_{S(0)}(\psi(0), 0) + \int_0^{t^*} \mu^{N(\sigma,t^*)} e^{-\rho(t^*-\sigma)} \|\varpi(\sigma)\|^2 d\sigma, \quad t^* \in [t_k, t_{k+1}). \quad (3.7)$$

For $t \in [t_{k+1}, t_{k+2})$, using (3.2) and (3.3) and noticing that $N(0, t) = k + 1$, one has

$$\begin{aligned} \mathcal{V}_{S(t)}(\psi(t), t) &= \mathcal{V}_{S(t_{k+1})}(\psi(t), t) \\ &\leq e^{-\rho(t-t_{k+1})} \mathcal{V}_{S(t_{k+1})}(\psi(t_{k+1}), t_{k+1}) + \int_{t_{k+1}}^t e^{-\rho(t-\sigma)} \|\varpi(\sigma)\|^2 d\sigma \\ &\leq \mu e^{-\rho(t-t_{k+1})} \mathcal{V}_{S(t_k)}(\psi(t_{k+1}), t_{k+1}) + \int_{t_{k+1}}^t e^{-\rho(t-\sigma)} \|\varpi(\sigma)\|^2 d\sigma \\ &= \mu e^{-\rho(t-t_{k+1})} \lim_{t^* \rightarrow t_{k+1}^-} \mathcal{V}_{S(t_k)}(\psi(t^*), t^*) + \int_{t_{k+1}}^t e^{-\rho(t-\sigma)} \|\varpi(\sigma)\|^2 d\sigma. \end{aligned}$$

It follows from (3.7) that

$$\begin{aligned}
& \mathcal{V}_{S(t)}(\psi(t), t) \\
& \leq \mu e^{-\rho(t-t_{k+1})} \lim_{r^* \rightarrow t_{k+1}^-} \left\{ \mu^{N(0, r^*)} e^{-\rho(r^*-0)} \mathcal{V}_{S(0)}(\psi(0), 0) + \int_0^{r^*} \mu^{N(\sigma, r^*)} e^{-\rho(r^*-\sigma)} \|\varpi(\sigma)\|^2 d\sigma \right\} \\
& \quad + \int_{t_{k+1}}^t e^{-\rho(t-\sigma)} \|\varpi(\sigma)\|^2 d\sigma \\
& = \lim_{r^* \rightarrow t_{k+1}^-} \left\{ \mu e^{-\rho(t-t_{k+1})} \mu^{N(0, r^*)} e^{-\rho(r^*-0)} \mathcal{V}_{S(0)}(\psi(0), 0) + \mu e^{-\rho(t-t_{k+1})} \int_0^{r^*} \mu^{N(\sigma, r^*)} e^{-\rho(r^*-\sigma)} \|\varpi(\sigma)\|^2 d\sigma \right\} \\
& \quad + \int_{t_{k+1}}^t e^{-\rho(t-\sigma)} \|\varpi(\sigma)\|^2 d\sigma \\
& = \mu^{N(0, t)} e^{-\rho t} \mathcal{V}_{S(0)}(\psi(0), 0) + \int_0^{t_{k+1}} \mu^{N(\sigma, t)} e^{-\rho(t-\sigma)} \|\varpi(\sigma)\|^2 d\sigma + \int_{t_{k+1}}^t \mu^{N(\sigma, t)} e^{-\rho(t-\sigma)} \|\varpi(\sigma)\|^2 d\sigma \\
& = \mu^{N(0, t)} e^{-\rho t} \mathcal{V}_{S(0)}(\psi(0), 0) + \int_0^t \mu^{N(\sigma, t)} e^{-\rho(t-\sigma)} \|\varpi(\sigma)\|^2 d\sigma,
\end{aligned}$$

which means that (3.6) holds true for $t \in [t_{k+1}, t_{k+2})$.

When $\varpi(t) = 0$, for $t > 0$, one obtains from (3.6) that

$$\mathcal{V}_{S(t)}(\psi(t), t) \leq \mu^{N(0, t)} e^{-\rho t} \mathcal{V}_{S(0)}(\psi(0), 0), \quad (3.8)$$

which, together with

$$0 \leq N(\sigma, t) \leq \left(\frac{t-\sigma}{\varepsilon+\delta} + 1 \right) (\delta/h_t + 1) \quad (3.9)$$

results in

$$\mathcal{V}_{S(t)}(\psi(t), t) \leq \mu^{\delta/h_t+1} e^{-\left(\rho - \frac{(\delta/h_t+1)\ln\mu}{\varepsilon+\delta}\right)t} \mathcal{V}_{S(0)}(\psi(0), 0). \quad (3.10)$$

From (3.5), one can find that

$$\rho - \frac{(\delta/h_t + 1) \ln \mu}{\varepsilon + \delta} \geq 0. \quad (3.11)$$

It follows from (3.1), (3.10) and (3.11) that

$$\begin{aligned}
\beta_1(\|\psi(t)\|) & \leq \mu^{\delta/h_t+1} e^{-\left(\rho - \frac{(\delta/h_t+1)\ln\mu}{\varepsilon+\delta}\right)t} \beta_2(\|\psi(0)\|) \\
& \leq \mu^{\delta/h_t+1} \beta_2(\|\psi(0)\|),
\end{aligned}$$

which means that

$$\|\psi(t)\| \leq \beta_1^{-1}(\mu^{\delta/h_t+1} \beta_2(\|\psi(0)\|)).$$

Thus, CTSS (2.1) is AS in light of Definition 1.

When $\varpi(t) \neq 0$, given that $\psi(0) = 0$, from (3.6), one has

$$\mathcal{V}_{S(t)}(\psi(t), t) \leq \int_0^t \mu^{N(\sigma, t)} e^{-\rho(t-\sigma)} \|\varpi(\sigma)\| d\sigma,$$

for any $t > 0$, which, together with (3.4), yields that

$$\|\phi(t)\|^2 \leq \gamma^2 \int_0^t \mu^{N(\sigma,t)} e^{-\rho(t-\sigma)} \|\varpi(\sigma)\|^2 d\sigma. \quad (3.12)$$

From (3.9)–(3.12), one has

$$\begin{aligned} \|\phi(t)\|^2 &\leq \gamma^2 \int_0^t \mu^{\left(\frac{t-\sigma}{\varepsilon+\delta}+1\right)(\delta/h_t+1)} e^{-\rho(t-\sigma)} \|\varpi(\sigma)\|^2 d\sigma \\ &= \gamma^2 \mu^{\delta/h_t+1} \int_0^t e^{-\left(\rho-\frac{(\delta/h_t+1)\ln\mu}{\varepsilon+\delta}\right)(t-\sigma)} \|\varpi(\sigma)\|^2 d\sigma \\ &\leq \bar{\gamma}^2 \int_0^t \|\varpi(\sigma)\|^2 d\sigma. \end{aligned}$$

Thus, CTSS (2.1) has the EPDAP level $\bar{\gamma}$ according to Definition 2.

Now, as in [40–42], we consider a state-feedback-based controller as

$$u(t) = K_{\varsigma(t)}\psi(t). \quad (3.13)$$

Based on Lemma 1, a design approach of the controller in (3.13) is given as follows:

Theorem 1. *Given scalars $\delta \geq 0$, $\mu > 1$, $\rho > 0$, $\gamma > 0$, $\theta > 0$ and $h_t > 0$, suppose that, for $i_1 \in \mathcal{M}$, there exist matrices $P_{i_1} > 0$, X_{i_1} and Y_{i_1} such that (3.5) and*

$$\begin{bmatrix} \Omega_1^1 & P_{i_1} E_{i_1} & \Omega_1^2 \\ * & -I & 0 \\ * & * & -\theta \mathcal{S}\{X_{i_1}\} \end{bmatrix} < 0, \quad (3.14)$$

$$P_{i_1} \leq \mu P_{i_2}, \quad (3.15)$$

$$\begin{bmatrix} -P_{i_1} & G_{i_1}^T \\ * & -\gamma^2 I \end{bmatrix} < 0 \quad (3.16)$$

hold, where

$$\begin{aligned} \Omega_1^1 &= \mathcal{S}\{P_{i_1} A_{i_1} + B_{i_1} Y_{i_1}\} + \rho P_{i_1}, \\ \Omega_1^2 &= P_{i_1} B_{i_1} - B_{i_1} X_{i_1} + \theta Y_{i_1}^T. \end{aligned}$$

Then, CTSS (2.1) is AS with the EPDAP level $\bar{\gamma} = \gamma \sqrt{\mu^{\delta/h_t+1}}$ if the controller gains are chosen as

$$K_{i_1} = X_{i_1}^{-1} Y_{i_1}, \quad i_1 \in \mathcal{M}. \quad (3.17)$$

Proof. Consider the LF

$$\mathcal{V}_{\varsigma(t)}(\psi(t), t) = \psi^T(t) P_{\varsigma(t)} \psi(t).$$

Under the conditions of $P_{i_1} > 0$, $P_{i_2} > 0$ and (3.15), the conditions (3.1) and (3.2) hold true. For any $\varsigma(t) = i_1$, taking the derivative along CTSS (2.1), we have

$$\dot{\mathcal{V}}_{i_1}(\psi(t), t) + \rho \mathcal{V}_{i_1}(\psi(t), t) - \|\varpi(t)\|^2$$

$$= \psi_{\varpi}^T(t) \Lambda_{i_1} \psi_{\varpi}(t),$$

where

$$\psi_{\varpi}^T(t) = \begin{bmatrix} \psi^T(t) & \varpi^T(t) \end{bmatrix},$$

$$\Lambda_{i_1} = \begin{bmatrix} \mathcal{S}\{P_{i_1}(A_{i_1} + B_{i_1}K_{i_1})\} + \rho P_{i_1} & P_{i_1}E_{i_1} \\ * & -I \end{bmatrix}.$$

Because $K_{i_1} = X_{i_1}^{-1}Y_{i_1}$, we can obtain that $\mathcal{S}\{P_{i_1}B_{i_1}K_{i_1}\} = \mathcal{S}\{B_{i_1}Y_{i_1} + (P_{i_1}B_{i_1} - B_{i_1}X_{i_1})X_{i_1}^{-1}Y_{i_1}\}$. Then, utilizing Proposition 2, from (3.14) we have that $\Lambda_{i_1} < 0$, which means that (3.3) is satisfied. Furthermore, by applying Proposition 3 to (3.16), (3.4) in Lemma 1 can be guaranteed. Thus, from Lemma 1, CTSS (2.1) is AS with the EPDAP level $\bar{\gamma}$.

The controller designed in (3.13) is time-independent. Next, we focus on the time-dependent design. The controller to be determined takes the form of

$$u(t) = K_{S(t), q_t} \psi(t), \quad (3.18)$$

where q_t is a time scheduler that takes values in $\mathcal{N} = \{0, \dots, \lfloor \varepsilon/h_t \rfloor\}$, described by

$$q_t = \begin{cases} \left\lfloor \frac{t-t_{m(r)}}{h_t} \right\rfloor, & t \in [t_{m(r)}, t_{m(r)} + \varepsilon), \\ \left\lfloor \frac{\varepsilon}{h_t} \right\rfloor, & t \in [t_{m(r)} + \varepsilon, t_{m(r)+1}), \\ \left\lfloor \frac{t-t_{\eta}}{h_t} \right\rfloor, & t \in [t_{m(r)+1}, t_{m(r+1)}) \end{cases} \quad (3.19)$$

with $t_{\eta} \triangleq \max_{t_i \in [0, t]} \{t_i\}$.

The following result can be deduced from Lemma 1.

Lemma 2. Given scalars $\delta \geq 0$, $\mu > 1$, $\rho > 0$, $\gamma > 0$ and $h_t > 0$, suppose that, for $t > 0$ and $r \in \mathbb{Z}_+$, there exists a QTD LF $\mathcal{V}_{S(t)}(\psi(t), q_t): (\mathbb{R}^n, \mathbb{Z}_+) \rightarrow \mathbb{R}$ and two classes of functions $\beta_1(\cdot), \beta_2(\cdot) \in \mathcal{K}_{\infty}$ such that

$$\beta_1(\|\psi(t)\|) \leq \mathcal{V}_{S(t)}(\psi(t), q_t) \leq \beta_2(\|\psi(t)\|), \quad (3.20)$$

$$\dot{\mathcal{V}}_{S(t)}(\psi(t), q_t) \leq -\rho \mathcal{V}_{S(t)}(\psi(t), q_t) + \|\varpi(t)\|^2, \quad (3.21)$$

$$\|\phi(t)\|^2 \leq \gamma^2 \mathcal{V}_{S(t)}(\psi(t), q_t), \quad (3.22)$$

$$\mathcal{V}_{S(t_{m(r)+1})}(\psi(t_{m(r)+\kappa}), 0) \leq \begin{cases} \mu \mathcal{V}_{S(t_{m(r)+\kappa}^-)}(\psi(t_{m(r)+\kappa}), M_{\varepsilon}), & \kappa = 1, \\ \mu \mathcal{V}_{S(t_{m(r)+\kappa}^-)}(\psi(t_{m(r)+\kappa}), M_{r, \kappa-1}), & \kappa = 2, \dots, n_r + 1 \end{cases} \quad (3.23)$$

hold, where

$$M_{\varepsilon} = \left\lfloor \frac{\varepsilon}{h_t} \right\rfloor, \quad M_{r, \kappa} = \left\lfloor \frac{\delta_{r, \kappa}}{h_t} \right\rfloor.$$

Then, for any PDT switching signal satisfying (3.5), CTSS (2.1) is AS with the EPDAP level $\bar{\gamma} = \gamma \sqrt{\mu^{\delta/h_t+1}}$.

Proof. Let $\check{\mathcal{V}}_{\mathcal{S}(t)}(\psi(t), t) = \mathcal{V}_{\mathcal{S}(t)}(\psi(t), q_t)$. Then, we deduce from (3.20)–(3.22) that

$$\begin{aligned}\beta_1(\|\psi(t)\|) &\leq \check{\mathcal{V}}_{\mathcal{S}(t)}(\psi(t), t) \leq \beta_2(\|\psi(t)\|), \\ \dot{\check{\mathcal{V}}}_{\mathcal{S}(t)}(\psi(t), t) &\leq -\rho\check{\mathcal{V}}_{\mathcal{S}(t)}(\psi(t), t) + \|\varpi(t)\|^2, \\ \|\phi(t)\|^2 &\leq \gamma^2\check{\mathcal{V}}_{\mathcal{S}(t)}(\psi(t), t),\end{aligned}$$

which correspond to (3.1), (3.3) and (3.4) in Lemma 1, respectively.

Next, we need to prove that

$$\check{\mathcal{V}}_{\mathcal{S}(t)}(\psi(t), t) \leq \mu\check{\mathcal{V}}_{\mathcal{S}(t^-)}(\psi(t), t) \quad (3.24)$$

holds, which corresponds to (3.2) in Lemma 1. Obviously (3.24) holds true when t is not a switching instant. When $t = t_{m(r)+1}$ ($r \in \mathbb{Z}_+$), from (3.23), we obtain

$$\begin{aligned}\check{\mathcal{V}}_{\mathcal{S}(t)}(\psi(t), t) &= \mathcal{V}_{\mathcal{S}(t_{m(r)+1})}(\psi(t_{m(r)+1}), q_{t_{m(r)+1}}) \\ &= \mathcal{V}_{\mathcal{S}(t_{m(r)+1})}(\psi(t_{m(r)+1}), 0) \\ &\leq \mu\mathcal{V}_{\mathcal{S}(t_{m(r)+1}^-)}(\psi(t_{m(r)+1}), M_\varepsilon) \\ &= \mu\mathcal{V}_{\mathcal{S}(t_{m(r)+1}^-)}(\psi(t_{m(r)+1}), q_{t_{m(r)+1}^-}) \\ &= \mu\check{\mathcal{V}}_{\mathcal{S}(t^-)}(\psi(t), t),\end{aligned}$$

and for $t = t_{m(r)+\kappa}$ ($\kappa = 2, \dots, n_r + 1$, $r \in \mathbb{Z}_+$), we have

$$\begin{aligned}\check{\mathcal{V}}_{\mathcal{S}(t)}(\psi(t), t) &= \mathcal{V}_{\mathcal{S}(t_{m(r)+\kappa})}(\psi(t_{m(r)+\kappa}), q_{t_{m(r)+\kappa}}) \\ &= \mathcal{V}_{\mathcal{S}(t_{m(r)+\kappa})}(\psi(t_{m(r)+\kappa}), 0) \\ &\leq \mu\mathcal{V}_{\mathcal{S}(t_{m(r)+\kappa}^-)}(\psi(t_{m(r)+\kappa}), M_{r, \kappa-1}) \\ &= \mu\mathcal{V}_{\mathcal{S}(t_{m(r)+\kappa}^-)}(\psi(t_{m(r)+\kappa}), q_{t_{m(r)+\kappa}^-}) \\ &= \mu\check{\mathcal{V}}_{\mathcal{S}(t^-)}(\psi(t), t).\end{aligned}$$

Thus, (3.24) also holds when t is a switching instant. The proof is finished.

Then, based on Lemma 2, the desired QTD controller can be constructed according to the following theorem.

Theorem 2. *Given scalars $\delta \geq 0$, $\mu > 1$, $\rho > 0$, $\gamma > 0$, $\theta > 0$ and $h_i > 0$, suppose that, for $i_1 \in \mathcal{M}$, $i_2 \in \{0, \dots, M_\varepsilon - 1\}$ and $i_3 \in \mathcal{M}$, there exist matrices $\tilde{P}_{i_1, i_2} > 0$, $\tilde{P}_{i_1, M_\varepsilon} > 0$, X_{i_1, i_2} , X_{i_1, M_ε} , Y_{i_1, i_2} and Y_{i_1, M_ε} satisfying*

$$\begin{bmatrix} \Psi_{i_1 i_2}^1 & \tilde{P}_{i_1, i_2} E_{i_1} & \tilde{P}_{i_1, i_2} B_{i_1} - B_{i_1} X_{i_1, i_2} + \theta Y_{i_1, i_2}^T \\ * & -I & 0 \\ * & * & -\theta \mathcal{L}\{X_{i_1, i_2}\} \end{bmatrix} < 0, \quad (3.25)$$

$$\begin{bmatrix} \Psi_{i_1 i_2}^2 & \tilde{P}_{i_1, i_2+1} E_{i_1} & \tilde{P}_{i_1, i_2+1} B_{i_1} - B_{i_1} X_{i_1, i_2} + \theta Y_{i_1, i_2}^T \\ * & -I & 0 \\ * & * & -\theta \mathcal{L}\{X_{i_1, i_2}\} \end{bmatrix} < 0, \quad (3.26)$$

$$\begin{bmatrix} \Psi_{i_1 M_\varepsilon}^3 & \tilde{P}_{i_1, M_\varepsilon} E_{i_1} & \tilde{P}_{i_1, M_\varepsilon} B_{i_1} - B_{i_1} X_{i_1, M_\varepsilon} + \theta Y_{i_1, M_\varepsilon}^T \\ * & -I & 0 \\ * & * & -\theta \mathcal{S}\{X_{i_1, M_\varepsilon}\} \end{bmatrix} < 0, \quad (3.27)$$

$$\begin{bmatrix} -\tilde{P}_{i_1, i_2} & G_{i_1}^T \\ * & -\gamma^2 I \end{bmatrix} < 0, \quad (3.28)$$

$$\begin{bmatrix} -\tilde{P}_{i_1, i_2+1} & G_{i_1}^T \\ * & -\gamma^2 I \end{bmatrix} < 0, \quad (3.29)$$

$$\begin{bmatrix} -\tilde{P}_{i_1, M_\varepsilon} & G_{i_1}^T \\ * & -\gamma^2 I \end{bmatrix} < 0, \quad (3.30)$$

and

$$\tilde{P}_{i_1, 0} \leq \mu \tilde{P}_{i_3, \kappa}, \quad \kappa = 0, 1, \dots, M_\varepsilon \quad (3.31)$$

for $i_1 \neq i_3$, where

$$\begin{aligned} \Psi_{i_1 i_2}^1 &= \mathcal{S}(\tilde{P}_{i_1, i_2} A_{i_1} + B_{i_1} Y_{i_1, i_2}) + \frac{1}{h_t} (\tilde{P}_{i_1, i_2+1} - \tilde{P}_{i_1, i_2}) + \rho \tilde{P}_{i_1, i_2}, \\ \Psi_{i_1 i_2}^2 &= \mathcal{S}(\tilde{P}_{i_1, i_2+1} A_{i_1} + B_{i_1} Y_{i_1, i_2}) + \frac{1}{h_t} (\tilde{P}_{i_1, i_2+1} - \tilde{P}_{i_1, i_2}) + \rho \tilde{P}_{i_1, i_2+1}, \\ \Psi_{i_1 M_\varepsilon}^3 &= \mathcal{S}(\tilde{P}_{i_1, M_\varepsilon} A_{i_1} + B_{i_1} Y_{i_1, M_\varepsilon}) + \rho \tilde{P}_{i_1, M_\varepsilon}. \end{aligned}$$

Then, for any PDT switching signal satisfying (3.5), the time-dependent controller in (3.18) can ensure that CTSS (2.1) is AS with the EPDAP level $\bar{\gamma} = \gamma \sqrt{\mu^{\delta/h_t+1}}$ if the control gains are chosen as

$$K_{i_1, i_2} = X_{i_1, i_2}^{-1} Y_{i_1, i_2}, \quad i_1 \in \mathcal{M}, \quad i_2 \in \mathcal{N}. \quad (3.32)$$

Proof. Define $\eta_{i_2} = i_2 h_t$. Then, the switching interval $[t_{m(r)}, t_{m(r+1)})$ can be reformulated as

$$[t_{m(r)}, t_{m(r+1)}) = \bigcup_{i_2=0}^{M_\varepsilon-1} [t_{m(r)} + \eta_{i_2}, t_{m(r)} + \eta_{i_2+1}) \cup [t_{m(r)} + \eta_{M_\varepsilon}, t_{m(r+1)}).$$

Consider the following LF

$$\mathcal{V}_{\zeta(t)}(\psi(t), q_t) = \psi^T(t) P(\zeta(t), q_t) \psi(t), \quad (3.33)$$

where

$$P(\zeta(t), q_t) = \begin{cases} \tilde{P}_{\zeta(t), q_t} + (\tilde{P}_{\zeta(t), q_t+1} - \tilde{P}_{\zeta(t), q_t}) \varphi(t), & t \in [t_{m(r)} + \eta_{q_t}, t_{m(r)} + \eta_{q_t+1}), \quad 0 \leq q_t \leq M_\varepsilon - 1, \\ \tilde{P}_{\zeta(t), M_\varepsilon}, & t \in [t_{m(r)} + \eta_{M_\varepsilon}, t_{m(r+1)}), \\ \tilde{P}_{\zeta(t), q_t} + (\tilde{P}_{\zeta(t), q_t+1} - \tilde{P}_{\zeta(t), q_t}) \varphi(t), & t \in [t_{m(r)+\kappa} + \eta_{q_t}, t_{m(r)+\kappa} + \eta_{q_t+1}), \quad 0 \leq q_t \leq M_{r, \kappa} - 1, \\ \tilde{P}_{\zeta(t), M_{r, \kappa}}, & t \in [t_{m(r)+\kappa} + \eta_{M_{r, \kappa}}, t_{m(r)+\kappa+1}), \end{cases}$$

$$\varphi(t) = \frac{t - (t_{m(r)+\kappa} + \eta_{q_t})}{h_t}, \quad \kappa = 1, 2, \dots, n_r.$$

Note that $\mathcal{V}_{\zeta(t)}(\psi(t), q_t)$ is continuous on $[t_{m(r)}, t_{m(r+1)})$ and differentiable at $t \neq t_{m(r)+\kappa}$. Obviously, (3.20) is satisfied. In addition, (3.23) is guaranteed by (3.31).

Next, we only need to show that (3.21) and (3.22) hold true for any $t \geq 0$. In order to simplify the notations, we take $\varsigma(t) = i_1$ and $q_t = i_2$. For any $r \in \mathbb{Z}_+$, when $t \in [t_{m(r)}, t_{m(r)} + \eta_{M_\varepsilon})$, we can get from (3.33) that

$$\mathcal{V}_{i_1}(\psi(t), i_2) = \psi^T(t) \left(\tilde{P}_{i_1, i_2} + \left(\tilde{P}_{i_1, i_2+1} - \tilde{P}_{i_1, i_2} \right) \varphi(t) \right) \psi(t). \quad (3.34)$$

Then, we obtain

$$\dot{\mathcal{V}}_{i_1}(\psi(t), i_2) = 2\psi^T(t) \left(\tilde{P}_{i_1, i_2} + \left(\tilde{P}_{i_1, i_2+1} - \tilde{P}_{i_1, i_2} \right) \varphi(t) \right) \dot{\psi}(t) + \frac{1}{h_t} \psi^T(t) \left(\tilde{P}_{i_1, i_2+1} - \tilde{P}_{i_1, i_2} \right) \psi(t). \quad (3.35)$$

According to CTSS (2.1) and (3.35), we have

$$\begin{aligned} & \dot{\mathcal{V}}_{i_1}(\psi(t), i_2) + \rho \mathcal{V}_{i_1}(\psi(t), i_2) - \|\varpi(t)\|^2 \\ &= 2\psi^T(t) \left(\tilde{P}_{i_1, i_2} + \left(\tilde{P}_{i_1, i_2+1} - \tilde{P}_{i_1, i_2} \right) \varphi(t) \right) \left((A_{i_1} + B_{i_1} K_{i_1, i_2}) \psi(t) + E_{i_1} \varpi(t) \right) + \rho \psi^T(t) \tilde{P}_{i_1, i_2} \psi(t) \\ & \quad + \rho \psi^T(t) \left(\tilde{P}_{i_1, i_2+1} - \tilde{P}_{i_1, i_2} \right) \varphi(t) \psi(t) + \frac{1}{h_t} \psi^T(t) \left(\tilde{P}_{i_1, i_2+1} - \tilde{P}_{i_1, i_2} \right) \psi(t) - \|\varpi(t)\|^2 \\ &= (1 - \varphi(t)) \left(\psi^T(t) \mathcal{S} \left(\tilde{P}_{i_1, i_2} (A_{i_1} + B_{i_1} K_{i_1, i_2}) \right) \psi(t) + \psi^T(t) \mathcal{S} \left(\tilde{P}_{i_1, i_2} E_{i_1} \right) \varpi(t) + \rho \psi^T(t) \tilde{P}_{i_1, i_2} \psi(t) \right. \\ & \quad \left. + \frac{1}{h_t} \psi^T(t) \left(\tilde{P}_{i_1, i_2+1} - \tilde{P}_{i_1, i_2} \right) \psi(t) - \|\varpi(t)\|^2 \right) + \varphi(t) \left(\psi^T(t) \mathcal{S} \left(\tilde{P}_{i_1, i_2+1} (A_{i_1} + B_{i_1} K_{i_1, i_2}) \right) \psi(t) \right. \\ & \quad \left. + \psi^T(t) \mathcal{S} \left(\tilde{P}_{i_1, i_2+1} E_{i_1} \right) \varpi(t) + \rho \psi^T(t) \tilde{P}_{i_1, i_2+1} \psi(t) - \|\varpi(t)\|^2 \right) \\ & \quad + \frac{1}{h_t} \psi^T(t) \left(\tilde{P}_{i_1, i_2+1} - \tilde{P}_{i_1, i_2} \right) \psi(t) \\ &= (1 - \varphi(t)) \psi_{\varpi}^T(t) \Theta_{1i_1 i_2} \psi_{\varpi}(t) + \varphi(t) \psi_{\varpi}^T(t) \Theta_{2i_1 i_2} \psi_{\varpi}(t), \end{aligned} \quad (3.36)$$

where

$$\begin{aligned} \Theta_{1i_1 i_2} &= \begin{bmatrix} \Theta_{1i_1 i_2}^1 & \tilde{P}_{i_1, i_2} E_{i_1} \\ * & -I \end{bmatrix}, \quad \Theta_{2i_1 i_2} = \begin{bmatrix} \Theta_{2i_1 i_2}^1 & \tilde{P}_{i_1, i_2+1} E_{i_1} \\ * & -I \end{bmatrix}, \\ \Theta_{1i_1 i_2}^1 &= \mathcal{S} \left(\tilde{P}_{i_1, i_2} (A_{i_1} + B_{i_1} K_{i_1, i_2}) \right) + \frac{1}{h_t} \left(\tilde{P}_{i_1, i_2+1} - \tilde{P}_{i_1, i_2} \right) + \rho \tilde{P}_{i_1, i_2}, \\ \Theta_{2i_1 i_2}^1 &= \mathcal{S} \left(\tilde{P}_{i_1, i_2+1} (A_{i_1} + B_{i_1} K_{i_1, i_2}) \right) + \frac{1}{h_t} \left(\tilde{P}_{i_1, i_2+1} - \tilde{P}_{i_1, i_2} \right) + \rho \tilde{P}_{i_1, i_2+1}. \end{aligned}$$

In addition, utilizing CTSS (2.1) and (3.34), we can get

$$\begin{aligned} & \|\phi(t)\|^2 - \gamma^2 \mathcal{V}_{i_1}(\psi(t), i_2) \\ &= \psi^T(t) G_{i_1}^T G_{i_1} \psi(t) - \gamma^2 \psi^T(t) \left(\tilde{P}_{i_1, i_2} + \left(\tilde{P}_{i_1, i_2+1} - \tilde{P}_{i_1, i_2} \right) \varphi(t) \right) \psi(t) \\ &= (1 - \varphi(t)) \psi^T(t) \left(G_{i_1}^T G_{i_1} - \gamma^2 \tilde{P}_{i_1, i_2} \right) \psi(t) + \varphi(t) \psi^T(t) \left(G_{i_1}^T G_{i_1} - \gamma^2 \tilde{P}_{i_1, i_2+1} \right) \psi(t). \end{aligned} \quad (3.37)$$

Similarly, when $t \in [t_{m(r)} + \eta_{M_\varepsilon}, t_{m(r)+1})$, we have from (3.33) that

$$\mathcal{V}_{i_1}(\psi(t), M_\varepsilon) = \psi^T(t) \tilde{P}_{i_1, M_\varepsilon} \psi(t).$$

This, together with CTSS (2.1), enables us to get that

$$\dot{\mathcal{V}}_{i_1}(\psi(t), M_\varepsilon) + \rho \mathcal{V}_{i_1}(\psi(t), M_\varepsilon) - \|\varpi(t)\|^2 = \psi_{\varpi}^T(t) \Theta_{3i_1 M_\varepsilon} \psi_{\varpi}(t), \quad (3.38)$$

$$\|\phi(t)\|^2 - \gamma^2 \mathcal{V}_{i_1}(\psi(t), M_\varepsilon) = \psi^T(t) \left(G_{i_1}^T G_{i_1} - \gamma^2 \tilde{P}_{i_1, M_\varepsilon} \right) \psi(t), \quad (3.39)$$

where

$$\Theta_{3i_1 M_\varepsilon} = \begin{bmatrix} \mathcal{S} \left(\tilde{P}_{i_1, M_\varepsilon} (A_{i_1} + B_{i_1} K_{i_1, M_\varepsilon}) \right) + \rho \tilde{P}_{i_1, M_\varepsilon} & \tilde{P}_{i_1, M_\varepsilon} E_{i_1} \\ * & -I \end{bmatrix}.$$

Utilizing Proposition 2, we can deduce from (3.25)–(3.27) that

$$\Psi_{1i_1 i_2} + \mathcal{S} \left(U_{1i_1 i_2} X_{i_1, i_2}^{-1} V_{i_1 i_2}^T \right) < 0, \quad (3.40)$$

$$\Psi_{2i_1 i_2} + \mathcal{S} \left(U_{2i_1 i_2} X_{i_1, i_2}^{-1} V_{i_1 i_2}^T \right) < 0, \quad (3.41)$$

$$\Psi_{3i_1 M_\varepsilon} + \mathcal{S} \left(U_{3i_1 M_\varepsilon} X_{i_1, M_\varepsilon}^{-1} V_{i_1 M_\varepsilon}^T \right) < 0, \quad (3.42)$$

where

$$\begin{aligned} \Psi_{1i_1 i_2} &= \begin{bmatrix} \Psi_{i_1 i_2}^1 & \tilde{P}_{i_1, i_2} E_{i_1} \\ * & -I \end{bmatrix}, \Psi_{2i_1 i_2} = \begin{bmatrix} \Psi_{i_1 i_2}^2 & \tilde{P}_{i_1, i_2+1} E_{i_1} \\ * & -I \end{bmatrix}, \Psi_{3i_1 i_2} = \begin{bmatrix} \Psi_{i_1 i_2}^3 & \tilde{P}_{i_1, M_\varepsilon} E_{i_1} \\ * & -I \end{bmatrix}, \\ U_{1i_1 i_2} &= \begin{bmatrix} \left(\tilde{P}_{i_1, i_2} B_{i_1} - B_{i_1} X_{i_1, i_2} \right)^T & 0 \end{bmatrix}^T, U_{2i_1 i_2} = \begin{bmatrix} \left(\tilde{P}_{i_1, i_2+1} B_{i_1} - B_{i_1} X_{i_1, i_2} \right)^T & 0 \end{bmatrix}^T, \\ U_{3i_1 M_\varepsilon} &= \begin{bmatrix} \left(\tilde{P}_{i_1, M_\varepsilon} B_{i_1} - B_{i_1} X_{i_1, M_\varepsilon} \right)^T & 0 \end{bmatrix}^T, V_{i_1 M_\varepsilon} = \begin{bmatrix} Y_{i_1, M_\varepsilon} & 0 \end{bmatrix}^T. \end{aligned}$$

From (3.32) and (3.40)–(3.42), we can obtain that $\Theta_{1i_1 i_2} < 0$, $\Theta_{2i_1 i_2} < 0$ and $\Theta_{3i_1 M_\varepsilon} < 0$, which, together with (3.36) and (3.38), ensure (3.21) for $t \in [t_{m(r)}, t_{m(r)+1})$. In addition, by means of Proposition 3, (3.28)–(3.30), (3.37) and (3.39) ensure (3.22) for $t \in [t_{m(r)}, t_{m(r)+1})$. Furthermore, due to the fact that $M_{r, \kappa} \leq M_\varepsilon$, (3.25)–(3.30) guarantee (3.21) and (3.22) for $t \in [t_{m(r)+1}, t_{m(r+1)})$. Thus, (3.21) and (3.22) hold true for any $t \in [t_{m(r)}, t_{m(r+1)})$. Considering the arbitrariness of r , by Lemma 2, CTSS (2.1) is shown to be AS with the EPDAP level $\bar{\gamma} = \gamma \sqrt{\mu^{\delta/h_t} + 1}$. The proof is finished.

Remark 2. As commonly reported in the literature on SSSs with PDT switching (see, e.g., [43–45], the design strategy proposed in Theorem 1 is time-independent. In order to reduce conservativeness, Theorem 2 presents a QTD design strategy by incorporating the time scheduler q_t effectively. The benefits of this approach will be demonstrated in Section 4. However, it may be worth noting that this improvement comes at the cost of increased computational complexity.

4. Example

Consider CTSS (2.1) subject to the following parameters:

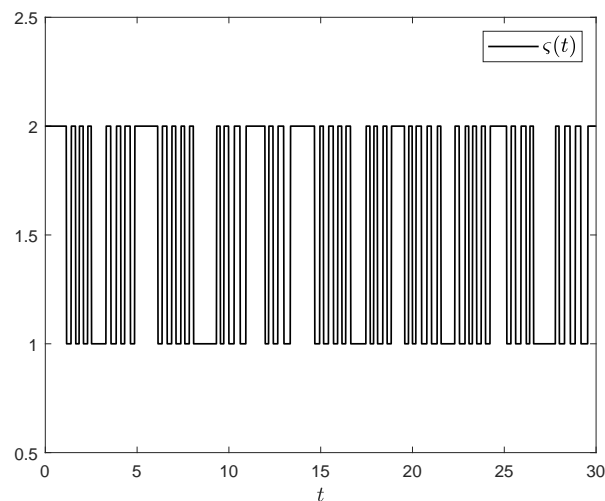
$$\begin{aligned} A_1 &= \begin{bmatrix} -0.5 & 0.6 \\ 0.83 & -0.55 \end{bmatrix}, B_1 = \begin{bmatrix} 0.1 \\ 0.28 \end{bmatrix}, \\ A_2 &= \begin{bmatrix} -0.6 & 0.55 \\ 0.5 & -0.3 \end{bmatrix}, B_2 = \begin{bmatrix} 0.1 \\ 0.2 \end{bmatrix}, \end{aligned}$$

Table 1. Optimal EPDAP level $\bar{\gamma}_{min}$ for different values of ρ given $\mu = 1.2$.

Method	$\bar{\gamma}_{min}$				
	$\rho = 0.1$	$\rho = 0.2$	$\rho = 0.3$	$\rho = 0.4$	$\rho = 0.5$
Theorem 1	0.0849	0.0990	0.1182	0.1463	0.1917
Theorem 2	0.0724	0.0837	0.0991	0.1210	0.1556

Table 2. Optimal EPDAP level $\bar{\gamma}_{min}$ for different values of μ given $\rho = 0.5$.

Method	$\bar{\gamma}_{min}$				
	$\mu = 1.25$	$\mu = 1.3$	$\mu = 1.35$	$\mu = 1.4$	$\mu = 1.45$
Theorem 1	0.2301	0.2741	0.3246	0.3821	0.4472
Theorem 2	0.1845	0.2180	0.2567	0.3010	0.3515

**Figure 2.** Trajectory of $\zeta(t)$.

$$E_1 = \begin{bmatrix} 0.1 \\ 0.1 \end{bmatrix}, E_2 = \begin{bmatrix} 0.5 \\ 0.5 \end{bmatrix},$$

$$G_1 = \begin{bmatrix} 0.1 & -0.1 \end{bmatrix}, G_2 = \begin{bmatrix} 0.2 & -0.2 \end{bmatrix}.$$

We set $\delta = 2$, $h_t = 0.2$ and $\theta = 0.1$. Then, by solving the LMIs of Theorems 1 and 2, respectively, we can get the comparison outcomes of the optimal EPDAP level $\bar{\gamma}_{min}$ for different values of ρ and μ , as described in Tables 1 and 2, respectively. From these two tables, we have two observations. First, when one of the values of ρ and μ is fixed, the optimal EPDAP level $\bar{\gamma}_{min}$ increases as the value of the other parameter increases. Second, when comparing the controller design method given in Theorem 1 with the one in Theorem 2, it is evident that the latter always yields better performance levels $\bar{\gamma}_{min}$. This improvement can be attributed to the fact that the design method in Theorem 2 is QTD.

Next, we set $\rho = 0.4$ and $\mu = 1.1$. By solving the LMIs of Theorem 2, we get the EPDAP level

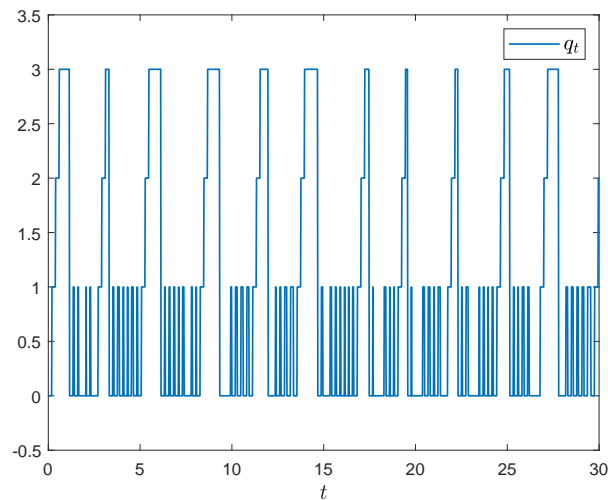


Figure 3. Trajectory of q_t .

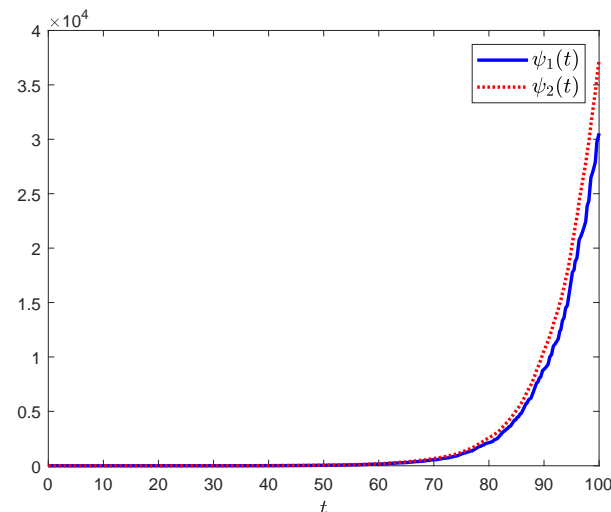


Figure 4. The trajectories of $\psi(t)$ for the open-loop CTSS.

$\bar{\gamma}_{min} = 0.0866$ and the controller gains as follows:

$$\begin{bmatrix} K_{1,0} & K_{1,1} \\ K_{1,2} & K_{1,3} \end{bmatrix} = \begin{bmatrix} -3.7775 & 0.5573 & -2.5836 & -0.7731 \\ -1.7309 & -1.7872 & -3.8081 & 1.3118 \end{bmatrix},$$

$$\begin{bmatrix} K_{2,0} & K_{2,1} \\ K_{2,2} & K_{2,3} \end{bmatrix} = \begin{bmatrix} -2.3377 & -0.4988 & -1.4927 & -1.4947 \\ -0.7562 & -2.3323 & -3.2563 & 0.2743 \end{bmatrix}.$$

In the simulation, we take the exterior disturbance as $\varpi(t) = e^{-0.2t} \sin(2t)$ and set the initial value as $\psi(0) = [5 \ -2]^T$. Figures 2–4 show the trajectories of PDT switching mode $\zeta(t)$, time scheduler q_t and states of the closed-loop CTSS, respectively. It is evident from Figure 4 that the open-loop CTSS is unstable. The trajectories of the states and control input of the closed-loop CTSS are depicted in Figure 5. It is apparent that the curves tend to zero as time $t \rightarrow \infty$, indicating that QTD controller (3.18) can ensure that the closed-loop CTSS is AS.

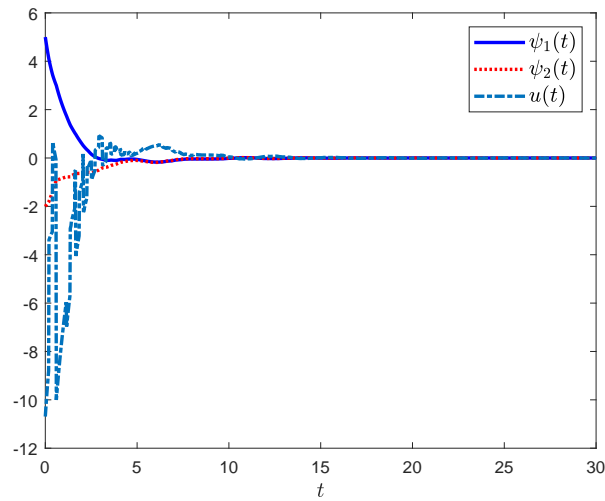


Figure 5. Trajectories of $\psi(t)$ and $u(t)$ for the closed-loop CTSS.

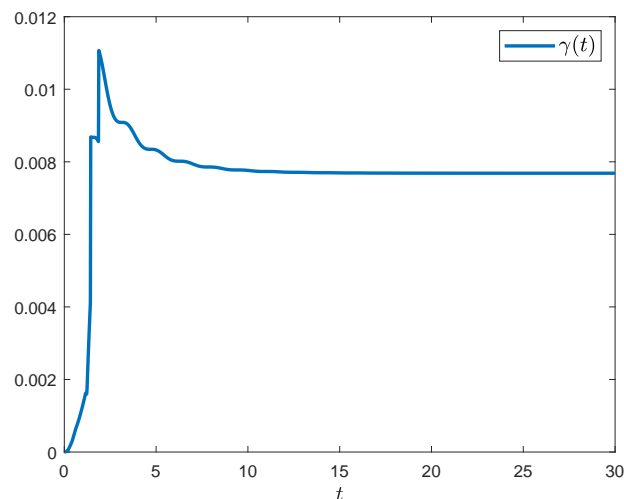


Figure 6. Trajectory of $\gamma(t)$.

At last, we introduce

$$\gamma(t) = \sqrt{\frac{\sup_{s \geq 0} \{\|\phi(s)\|^2\}}{\int_0^t \|\varpi(s)\|^2 ds}}.$$

Figure 6 further describes the curve of $\gamma(t)$ given that $\psi(0) = [0 \ 0]^T$. Apparently, $\gamma(t)$ progressively converges to 0.0077, which is smaller than the optimal EPDAP level $\bar{\gamma}_{min} = 0.0866$. This shows the effectiveness of controller (3.18) in ensuring the EPDAP of the closed-loop CTSS.

5. Conclusions

This work investigated the issue of energy-to-peak control for CTSSs with PDT switching. With the aid of an LF and a few decoupling techniques, a time-independent controller design approach

was proposed in Theorem 1. To reduce conservatism, a QTD controller design method was further presented in Theorem 2. The required gains of these two types of controllers can be acquired by solving LMIs. Finally, an example was utilized to illustrate the validity of our controller design approaches.

The controllers under consideration are based on full-state feedback, which utilizes state variables as feedback signals to generate control inputs. However, there are certain scenarios in which implementing such controllers becomes challenging because directly measuring all of the state variables is often difficult [46]. The issue of energy-to-peak control for CTSSs with PDT switching based on output feedback will be explored as an extension of the current work.

Use of AI tools declaration

The authors declare they have not used Artificial Intelligence (AI) tools in the creation of this article.

Conflict of interest

The authors declare there is no conflict of interest.

References

1. D. Liberzon, A. S. Morse, Basic problems in stability and design of switched systems, *IEEE Control Syst. Mag.*, **19** (1999), 59–70. <https://doi.org/10.1109/37.793443>
2. L. Zhang, X. Lou, Z. Wang, Output-based robust switching rule design for uncertain switched affine systems: Application to DC–DC converters, *IEEE Trans. Circuits Syst. II, Exp. Briefs*, **69** (2022), 4493–4497. <https://doi.org/10.1109/TCSII.2022.3183192>
3. T. Sun, R. Wang, L. Zhang, X. Zhao, A fastly and slowly cyclic switching strategy for discrete-time cyclic switched systems and its application to inverter circuits, *IEEE Trans. Circuits Syst. II, Exp. Briefs*, **69** (2022), 1173–1177. <https://doi.org/10.1109/TCSII.2021.3099160>
4. Z. Ye, D. Zhang, Z. G. Wu, H. Yan, A3C-based intelligent event-triggering control of networked nonlinear unmanned marine vehicles subject to hybrid attacks, *IEEE Trans. Intell. Transp. Syst.*, **23** (2022), 12921–12934. <https://doi.org/10.1109/TITS.2021.3118648>
5. F. Zhu, F. Wang, L. Ye, Artificial switched chaotic system used as transmitter in chaos-based secure communication, *J. Franklin Inst.*, **357** (2020), 10997–11020. <https://doi.org/10.1016/j.jfranklin.2020.07.043>
6. Y. Garbouj, T. N. Dinh, T. Raissi, T. Zouari, M. Ksouri, Optimal interval observer for switched Takagi–Sugeno systems: An application to interval fault estimation, *IEEE Trans. Fuzzy Syst.*, **29** (2021), 2296–2309. <https://doi.org/10.1109/TFUZZ.2020.2997333>
7. H. Wang, X. Yang, Z. Xiang, R. Tang, Q. Ning, Synchronization of switched neural networks via attacked mode-dependent event-triggered control and its application in image encryption, *IEEE Trans. Cybern.*, **2022** (2022). <https://doi.org/10.1109/TCYB.2022.3227021>
8. L. Zhang, X. Zhang, Y. Xue, X. Zhang, New method to global exponential stability analysis for switched genetic regulatory networks with mixed delays, *IEEE Trans. Nanobiosci.*, **19** (2020), 308–314. <https://doi.org/10.1109/TNB.2020.2971548>

9. M. Sathishkumar, Y. C. Liu, Resilient annular finite-time bounded and adaptive event-triggered control for networked switched systems with deception attacks, *IEEE Access*, **9** (2021), 92288–92299. <https://doi.org/10.1109/ACCESS.2021.3092402>
10. R. Vadivel, S. Sabarathinam, Y. Wu, K. Chaisena, N. Gunasekaran, New results on T-S fuzzy sampled-data stabilization for switched chaotic systems with its applications, *Chaos, Solitons & Fractals*, **164** (2022), 112741. <https://doi.org/10.1016/j.chaos.2022.112741>
11. H. Ji, Y. Li, X. Ding, J. Lu, Stability analysis of Boolean networks with Markov jump disturbances and their application in apoptosis networks, *Electron. Res. Arch.*, **30** (2022), 3422–3434. <https://doi.org/10.3934/era.2022174>
12. N. Gunasekaran, M. S. Ali, S. Arik, H. A. Ghaffar, A. A. Z. Diab, Finite-time and sampled-data synchronization of complex dynamical networks subject to average dwell-time switching signal, *Neural Networks*, **149** (2022), 137–145. <https://doi.org/10.1016/j.neunet.2022.02.013>
13. W. Tai, X. Li, J. Zhou, S. Arik, Asynchronous dissipative stabilization for stochastic Markov-switching neural networks with completely-and incompletely-known transition rates, *Neural Networks*, **161** (2023), 55–64. <https://doi.org/10.1016/j.neunet.2023.01.039>
14. J. Zhou, D. Xu, W. Tai, C. K. Ahn, Switched event-triggered \mathcal{H}_∞ security control for networked systems vulnerable to aperiodic DoS attacks, *IEEE Trans. Network Sci. Eng.*, **10** (2023), 2109–2123. <https://doi.org/10.1109/TNSE.2023.3243095>
15. R. Sakthivel, S. Harshavarthini, S. Mohanapriya, O. Kwon, Disturbance rejection based tracking control design for fuzzy switched systems with time-varying delays and disturbances, *Int. J. Robust Nonlinear Control*, **33** (2023), 1184–1202. <https://doi.org/10.1002/rnc.6419>
16. S. Cong, Mode-independent switching stabilizing control for continuous-time linear Markovian switching systems, *IEEE Trans. Autom. Control*, **2023** (2023). <https://doi.org/10.1109/TAC.2023.3255139>
17. H. Lin, P. J. Antsaklis, Stability and stabilizability of switched linear systems: A survey of recent results, *IEEE Trans. Autom. Control*, **54** (2009), 308–322. <https://doi.org/10.1109/TAC.2008.2012009>
18. A. S. Morse, Supervisory control of families of linear set-point controllers-Part I. exact matching, *IEEE Trans. Autom. Control*, **41** (1996), 413–431. <https://doi.org/10.1109/9.539424>
19. J. P. Hespanha, A. S. Morse, Stability of switched systems with average dwell-time, in *Proceedings of the 38th IEEE conference on decision and control (Cat. No. 99CH36304)*, **3** (1999), 2655–2660. <https://doi.org/10.1109/CDC.1999.831330>
20. J. P. Hespanha, Uniform stability of switched linear systems: Extensions of Lasalle’s invariance principle, *IEEE Trans. Autom. Control*, **49** (2004), 470–482. <https://doi.org/10.1109/TAC.2004.825641>
21. L. Zhang, S. Zhuang, P. Shi, Y. Zhu, Uniform tube based stabilization of switched linear systems with mode-dependent persistent dwell-time, *IEEE Trans. Autom. Control*, **60** (2015), 2994–2999. <https://doi.org/10.1109/TAC.2015.2414813>

22. H. Shen, M. Xing, Z. G. Wu, J. H. Park, Fault-tolerant control for fuzzy switched singular systems with persistent dwell-time subject to actuator fault, *Fuzzy Sets Syst.*, **392** (2020), 60–76. <https://doi.org/10.1016/j.fss.2019.08.011>
23. Y. Zhu, W. Zheng, D. Zhou, Quasi-synchronization of discrete-time Lur'e-type switched systems with parameter mismatches and relaxed PDT constraint, *IEEE Trans. Cybern.*, **50** (2020), 2026–2037. <https://doi.org/10.1109/TCYB.2019.2930945>
24. J. Wang, X. Liu, J. Xia, H. Shen, J. H. Park, Quantized interval type-2 fuzzy control for persistent dwell-time switched nonlinear systems with singular perturbations, *IEEE Trans. Cybern.*, **52** (2022), 6638–6648. <https://doi.org/10.1109/TCYB.2021.3049459>
25. N. Zhang, G. Chen, \mathcal{L}_1 finite-time control of discrete-time switched positive linear systems with mode-dependent persistent dwell-time switching, *Optim. Control Appl. Methods*, **43** (2022), 1778–1794. <https://doi.org/10.1002/oca.2928>
26. X. Q. Zhao, S. Guo, Y. Long, G. X. Zhong, Simultaneous fault detection and control for discrete-time switched systems under relaxed persistent dwell time switching, *Appl. Math. Comput.*, **412** (2022), 126585. <https://doi.org/10.1016/j.amc.2021.126585>
27. T. Yu, Y. Zhao, J. Wang, J. Liu, Event-triggered sliding mode control for switched genetic regulatory networks with persistent dwell time, *Nonlinear Anal. Hybrid Syst.*, **44** (2022), 101135. <https://doi.org/10.1016/j.nahs.2021.101135>
28. S. Zhuang, H. Gao, Y. Shi, Model predictive control of switched linear systems with persistent dwell-time constraints: Recursive feasibility and stability, *IEEE Trans. Autom. Control*, **2023** (2023). <https://doi.org/10.1109/TAC.2023.3248279>
29. H. Zhang, X. Zhang, J. Wang, Robust gain-scheduling energy-to-peak control of vehicle lateral dynamics stabilisation, *Veh. Syst. Dyn.*, **52** (2014), 309–340. <https://doi.org/10.1080/00423114.2013.879190>
30. L. Wu, Z. Wang, Robust $L_2 - L_\infty$ control of uncertain differential linear repetitive processes, *Syst. Control Lett.*, **57** (2008), 425–435. <https://doi.org/10.1016/j.sysconle.2007.10.005>
31. Y. Li, M. Chen, T. Li, H. Wang, Robust resilient control based on multi-approximator for the uncertain turbofan system with unmeasured states and disturbances, *IEEE Trans. Syst., Man Cybern.: Syst.*, **51** (2021), 6040–6049. <https://doi.org/10.1109/TSMC.2019.2958861>
32. J. Zhou, J. Dong, S. Xu, Asynchronous dissipative control of discrete-time fuzzy Markov jump systems with dynamic state and input quantization, *IEEE Trans. Fuzzy Syst.*, **2023** (2023). <https://doi.org/10.1109/TFUZZ.2023.3271348>
33. S. Shi, Z. Shi, Z. Fei, Asynchronous control for switched systems by using persistent dwell time modeling, *Syst. Control Lett.*, **133** (2019), 104523. <https://doi.org/10.1016/j.sysconle.2019.104523>
34. Y. Tong, W. Sun, X. Li, Discretized quasi-time-dependent \mathcal{H}_∞ control for continuous-time switched linear systems with persistent dwell-time, *Int. J. Robust Nonlinear Control*, **31** (2021), 3195–3211. <https://doi.org/10.1002/rnc.5444>

35. X. H. Chang, J. H. Park, P. Shi, Fuzzy resilient energy-to-peak filtering for continuous-time nonlinear systems, *IEEE Trans. Fuzzy Syst.*, **25** (2017), 1576–1588. <https://doi.org/10.1109/TFUZZ.2016.2612302>
36. L. Zhang, S. Zhuang, P. Shi, Non-weighted quasi-time-dependent \mathcal{H}_∞ filtering for switched linear systems with persistent dwell-time, *Automatica*, **54** (2015), 201–209. <https://doi.org/10.1016/j.automatica.2015.02.010>
37. R. Temam, *Infinite-Dimensional Dynamical Systems in Mechanics and Physics*, Springer, New York, USA, 2015. <https://doi.org/10.1007/978-1-4684-0313-8>
38. J. Zhou, J. H. Park, H. Shen, Non-fragile reduced-order dynamic output feedback \mathcal{H}_∞ control for switched systems with average dwell-time switching, *Int. J. Control*, **89** (2016), 281–296. <https://doi.org/10.1080/00207179.2015.1075175>
39. S. Boyd, L. E. Ghaoui, E. Feron, V. Balakrishnan, *Linear Matrix Inequalities in System and Control Theory*, SIAM, Philadelphia, USA, 1994. <https://doi.org/10.1137/1.9781611970777>
40. B. Kaviarasan, O. M. Kwon, M. J. Park, R. Sakthivel, Dissipative constraint-based control design for singular semi-Markovian jump systems using state decomposition approach, *Nonlinear Anal. Hybrid Syst.*, **47** (2023), 101302. <https://doi.org/10.1016/j.nahs.2022.101302>
41. X. Liu, K. Shi, Y. Tang, L. Tang, Y. Wei, Y. Han, A novel adaptive event-triggered reliable \mathcal{H}_∞ control approach for networked control systems with actuator faults, *Electron. Res. Arch.*, **31** (2023), 1840–1862. <https://doi.org/10.3934/era.2023095>
42. V. B. Falchetto, M. Souza, A. R. Fioravanti, R. N. Shorten, \mathcal{H}_2 and \mathcal{H}_∞ analysis and state feedback control design for discrete-time constrained switched linear systems, *Int. J. Control*, **94** (2021), 2834–2845. <https://doi.org/10.1080/00207179.2020.1737331>
43. Y. Guo, J. Li, X. Qi, Fault-tolerant \mathcal{H}_∞ control for T–S fuzzy persistent dwell-time switched singularly perturbed systems with time-varying delays, *Int. J. Fuzzy Syst.*, **24** (2022), 247–264. <https://doi.org/10.1007/s40815-021-01133-7>
44. H. Shen, Z. Huang, X. Yang, Z. Wang, Quantized energy-to-peak state estimation for persistent dwell-time switched neural networks with packet dropouts, *Nonlinear Dyn.*, **93** (2018), 2249–2262. <https://doi.org/10.1007/s11071-018-4322-y>
45. H. Shen, X. Liu, J. Xia, X. Chen, J. Wang, Finite-time energy-to-peak fuzzy filtering for persistent dwell-time switched nonlinear systems with unreliable links, *Inf. Sci.*, **579** (2021), 293–309. <https://doi.org/10.1016/j.ins.2021.07.081>
46. S. Dong, Z. G. Wu, P. Shi, *Control and Filtering of Fuzzy Systems with Switched Parameters*, Springer, New York, USA, 2020. <https://doi.org/10.1007/978-3-030-35566-1>



AIMS Press

©2023 the Author(s), licensee AIMS Press. This is an open access article distributed under the terms of the Creative Commons Attribution License (<http://creativecommons.org/licenses/by/4.0>)